Journal of Composite Materials

http://jcm.sagepub.com

Essential Work of Fracture and Acoustic Emission Study on TPNR Composites Reinforced by Kenaf Fiber

H. Anuar, S.H. Ahmad, R. Rasid, S.N. Surip, T. Czigany and G. Romhany

Journal of Composite Materials 2007; 41; 3035
DOI: 10.1177/0021998307082173

Essential Work of Fracture and Acoustic Emission Study on TPNR Composites Reinforced by Kenaf Fiber

H. ANUAR,* S. H. AHMAD, R. RASID AND S. N. SURIP
School of Applied Physics, Faculty of Science and Technology
Universiti Kebangsaan Malaysia, 43600 Bangi
Selangor Darul Ehsan, Malaysia

T. CZIGANY AND G. ROMHANY
Faculty of Mechanical Engineering, Department of Polymer Engineering
Budapest University of Technology and Economics
Muegyetem rkp. 3, H-1111 Budapest, Hungary

ABSTRACT: Kenaf fiber (KF) based thermoplastic natural rubber (TPNR) composite was produced by melt blending with polypropylene (PP). Kenaf fiber (15% by volume) and TPNR were mixed in as Haake 600p internal mixer. The fracture behavior of the TPNR matrix and of TPNR–kenaf (with and without maleic anhydride grafted polypropylene, MAPP) composites was evaluated using the essential work of fracture (EWF) method and double edge notched tensile (DENT) specimens. Various ligament lengths were employed ranging from 4 to 12 mm. The strain rate was fixed at 2 mm/min. The specific work of fracture (w_e) and plastic work (βw_p) showed the highest energy for TPNR that corresponds to its ductility and allows the application of the EWF approach. It was found that the presence of kenaf fibers and MAPP reduced the toughness of TPNR and changed the ductile fracture to brittle behavior. SEM observation revealed that energy absorption mechanisms include matrix deformation, fiber pullout, and fiber breakage. Acoustic emission (AE) was employed to analyze the failure processes further. The signals emitted by composites were substantially higher than that of the TPNR matrix, reflecting that also the failure mechanisms were affected by the fibers incorporated.

KEY WORDS: thermoplastic natural rubber, kenaf fiber, essential work of fracture, acoustic emission.

INTRODUCTION

THERMOPLASTIC NATURAL RUBBER (TPNR) is known as a blend of natural rubber and a polyolefin. Its properties are between that of rubber and plastic. The advantage of

*Author to whom correspondence should be addressed. E-mail: hazleenanuar@yahoo.com
Figure 6 appears in color online: http://jcm.sagepub.com

0021-9983/07/25 3035–15 $10.00/0 DOI: 10.1177/0021998307082173

TPNR is that it can be processed using any thermoplastic machinery at comparable prices [1]. It is benefited by adding a filler or reinforcement into the TPNR since it may reduce price and increase the performance, as well [2].

The use of thermoplastics possess several limitations as compared to it thermosetting counterpart, and furthermore the increasing prices of plastics and natural rubber have risen sharply over the past few years. Hence, effort is currently being made to combine natural fibers with thermoplastic elastomers which can provide cost reduction to the plastic industry. This simultaneously increased the value added of the lignocellulosic fibers. Lignocellulosic fiber offers various advantages including environmental friendly and decreasing wear of manufacturing machinery. Additionally, by careful selection of agro-fibers, considerable reinforcement of the plastic can be achieved by enhancing the mechanical properties of the composites during its useful lifetime. To a lesser extent, combination of TPNR and kenaf fiber were never studied and documented.

Kenaf fiber (KF) extracted from *Hibiscus cannabinus* L. plant is receiving attention in combining its fibers with thermoplastics in a way to develop a new type of composite. Apart from environmentally friendly, KF are also lower in density, inexpensive, biodegradable and has fairly good mechanical properties [3]. The KF derived from renewable resources is suitable for use in automotive applications, building appliance, etc.

Previous studies have shown that carbon and kenaf fiber exhibited low stress–strain to failure [3]. This behavior will cause fracture in composite materials and occurs catastrophically without warning. Therefore, composite based rubber-toughened polymer matrix will provide extra toughness and delay the failure with some mechanism dispersed through the material. The failure behavior in advanced materials and modern technologies particularly in transportation and building may expose everyday lives to high risk. However, the risk and failure can be minimized through fracture toughness studies and non-destructive evaluation.

Fracture toughness of polymers can be evaluated using the essential work of fracture (EWF) and J-integral method [4]. However, the EWF method has been gaining attention lately for the toughness description of ductile polymers, toughened polymer blends, and composites, because of the simplicity of the experimental process and data manipulation [5–10]. Previous researchers have studied the EWF response of various polymeric materials as a function of testing conditions, including specimen thickness [10,11], strain rate [11–13], temperature [14,15], influence of notching, moulding conditions [16], effect of physical ageing, plasticization [17], and molecular weight [18,19].

Acoustic emission (AE) techniques for non-destructive evaluation of material failure have been extensively used to study the fracture behavior of composite materials. It was demonstrated that monitoring AE during loading composites is a useful tool to identify the mechanisms of failure and to estimate the development of the damage zone [20].

Although the damage mechanisms in synthetic fiber reinforced polymer composites have been successfully monitored by AE before, according to the author's knowledge there have been no reports on acoustic emission associated with the damage mechanisms in reinforced TPNR. This article explores a new method to evaluate the fracture toughness of thermoplastic natural rubber TPNR reinforced by KF via the EWF method. The morphological analysis of the EWF fracture samples is also discussed. *In situ* monitoring of AE during EWF has been adopted to characterize the failure mechanism of TPNR–KF composites.

EXPERIMENTAL

Materials

Kenaf bast fiber (KF) was obtained from Livestock Strategic Research Centre (MARDI), Serdang. Polymers used were SMR-L grade natural rubber (NR) purchased from Rubber Research Industries Malaysia with density of 0.92 g/cm^3, polypropylene (PP) with a density of 0.905 g/cm^3 was supplied by Polipropilinas (M) Sdn. Bhd. and maleic anhydride polypropylene (MAPP) with a density of 0.95 g/cm^3 was from Aldrich Chemical Co. Liquid natural rubber (LNR) was synthesized using a photochemical oxidation technique on natural rubber in our laboratory [21].

Kenaf Fiber Preparation

Kenaf bast fibers were used in the form of flakes and sieved at 300–500 μm aperture sizes based on the optimum tensile results. The density of Kenaf fiber was measured to be 1.13 g/cm^3 and the moisture content was 4.1%.

Thermoplastic Natural Rubber Matrix Preparation

TPNR was melt blended using an internal mixer, Thermo Haake 600p. Mixtures of NR, LNR and PP at a ratio of 20 : 10 : 70 were used in this work. Blending was carried out at 175°C and at a rotor speed of 40 rpm for 12 min.

Composite Preparation

TPNR–KF composite were prepared using the same internal mixer. Prior to mixing, TPNR and KF were pre-mixed. MAPP (6%) was pre-mixed together with TPNR and KF whenever the use of coupling agent was required. Based on optimum processing parameters determination, mixing was carried out at 175°C for 12 min at a rotation speed of 9 rpm. The compound was then compression moulded for 16 min at 175°C.

Essential Work of Fracture (EWF)

According to Mai and Cotterell [22] and Wu and Mai [23], EWF is preferred when dealing with ductile and toughened polymer. Theoretically, EWF can be described as:

$$W_f = W_e + W_p \tag{1}$$

where W_e is the essential work of fracture and W_p is the non-essential or plastic work. Equation (1) can be rewritten as [7]:

$$W_f = w_e t l + \beta w_p t l^2 \tag{2}$$

where w_e and w_p are the specific essential work of fracture and specific plastic work, respectively. t is the thickness of the specimen, l is the ligament length, and β is the plastic zone shape factor. Thus, the specific total fracture work, w_f, is:

$$w_f = \frac{W_f}{tl} = w_e + \beta w_p l. \tag{3}$$

In Equation (3), w_e is the fracture toughness of the material.

Based on ESIS TC-4 Testing Protocol 28 [7], the EWF was used as a tool to evaluate fracture toughness of TPNR and TPNR–kenaf composites. The overall fiber content was 15% by volume. Samples were tested using a Zwick Z020 tensile tester at 2 mm/min strain rate. Five specimens were tested for each ligament length. DENT specimen geometry was employed. Pre-notching was done by cutting with a fresh razor blade. As described in the testing protocol, the EWF is independent of specimen geometry. The sample gauge lengths were varied among 4, 6, 8, 10, and 12 mm, while width and thickness were 30 mm and 1 mm, respectively. Details of the specimen geometry are described in Figure 1. The EWF fracture surfaces of the composites were observed under a scanning electron microscope (JEOL JSM-6380LA).

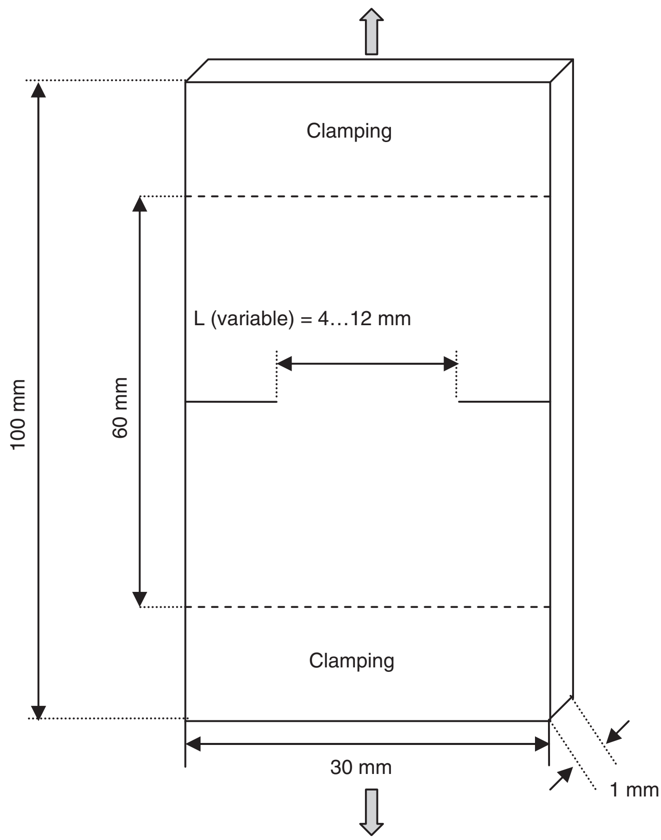

Figure 1. *Dimension of the DEN-T specimen for the EWF method.*

Acoustic Emission (AE) Tests

In order to obtain a deeper understanding of the failure behavior, the AE signals of the DENT specimens were recorded *in situ* using a miniature sensor (10 mm diameter) attached to the specimen surface and coupled to a SENSOPHONE AED-40/12 (Hungary). An A-11 type microphone, which operates on a piezo-electric basis, was fixed on the fracture mechanical specimens so that the sound waves could be detected. During the tests, the following primary AE signals were measured, calculated and stored: elapsed time, number of events, peak amplitude, event width, and rise time. The principle of this test is that the structure exposed to mechanical loading emits sound waves from the areas where any physical change (e.g., matrix deformation, fiber breakage, etc.) occurs. Different failure modes were assigned to the different signal levels determined based on the force–displacement curve and the physical parameters of the sound waves.

The AE technique aims at detecting and analyzing the sound waves emerging in the material in order to locate their origin as precisely as possible. For this purpose, a sensor (b) operating in the ultrasound range is fixed on the material (a) during loading. The recorded acoustic signals are amplified (c) and are processed with capable electronic systems (d), and then are analyzed with adequate software on a computer (e). Details of the schematic diagram of AE device is described in Figure 2.

RESULTS AND DISCUSSION

Tensile strength and tensile modulus of TPNR and reinforced TPNR by kenaf fiber are given in Table 1. Generally, the incorporation of kenaf fiber (with and without MAPP) into TPNR matrix has increased the tensile properties. Tensile strength for untreated TPNR–KF (UTK) and treated TPNR–KF (TK) were about 18% and 46% higher than unreinforced TPNR. The higher tensile properties obtained in TK are due to chemical linkages between hydroxyl group– coupling agent–matrix [3].

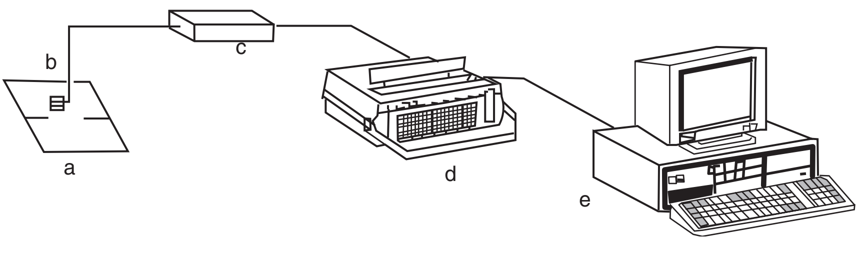

Figure 2. *Schematic diagram of AE measurement set-up.*

Table 1. Tensile properties (ASTM D638) of TPNR-KF at 15% by volume.

Materials	Tensile strength (MPa)	Tensile modulus (MPa)
TPNR	18.8	315
TPNR-UTK	22.1	524
TPNR-TK	27.5	676

Essential Work of Fracture (EWF)

The fracture resistance of TPNR blend and TPNR–kenaf composites in the presence of sharp cracks were evaluated by the EWF method. As shown in Figure 3, the TPNR curves exhibited a peak load, which corresponds to gross yielding, while beyond the maximum load, a slow decrease is observed indicating a slow stable crack that propagated perpendicular to the load direction. Besides, similarities in the load–displacement curves, as displayed in Figure 3, for each ligament length, were observed during the deformation process. The maximum load and the displacement at failure also increased with increasing ligament length. This shows that TPNR fulfilled one of the basic requirements of the EWF method. Figure 3 also ensures that the cracks propagated under similar stress conditions, being unchanged with the ligament length. The curves obtained for TPNR in Figure 3 were expected and successfully measured using the EWF method. This is due to the fact that the brittle behavior of PP has been toughened by 30% of natural rubber and hence TPNR underwent plastic deformation. DENT specimen of pure PP exhibited brittle behavior in the presence of notches, and thus EWF method is not suitable for pure PP (Tjong et al. [24]). The results obtained agreed with the previous studies by Li et al. [25] on elastomer-modified polypropylene and Mouzakis et al. [9] on elastomeric polypropylene (ELPP), who have successfully characterized fracture toughness via the EWF method.

The incorporation of kenaf fiber into TPNR has changed the fracture behavior of TPNR blends. The load–displacement curves for TPNR–KF composites are depicted in Figures 4 and 5. Figures 4 and 5 also show that the plastic zone has significantly diminished as demonstrated in Figure 3 for the TPNR matrix. In these cases the EWF approach cannot be applied for the determination of fracture mechanism for the reinforced TPNR. The criteria of yielding, necking and stable fracture propagation were always met in the case of the TPNR matrix examined (Figure 3). As can be seen in Figure 4 and 5, in the case of reinforced TPNR by kenaf fiber (with and without MAPP), the condition fulfilled the EWF requirements less and less. However, our aim was to

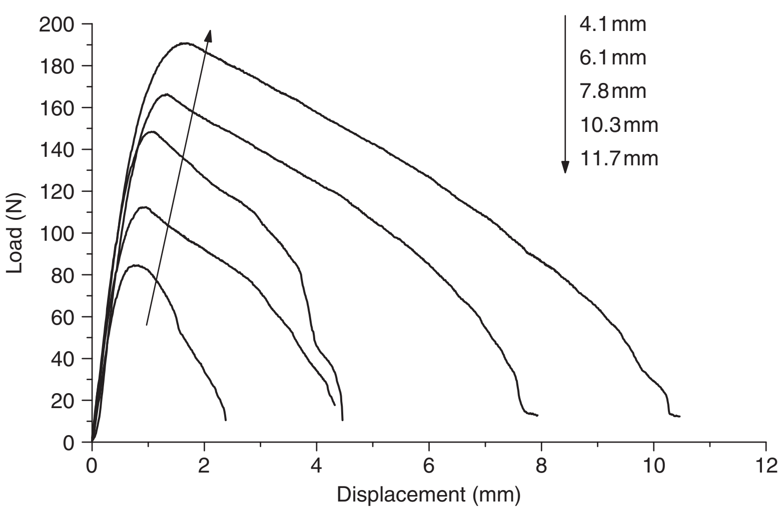

Figure 3. *Load–displacement curves for TPNR matrix.*

investigate the impact of kenaf fiber reinforcement, and the results obtained for fiber reinforcement can only be used for comparison with the matrix in our case.

Specific work of fracture (w_f) versus ligament length for TPNR and kenaf composites is shown in Figure 6, which reveals that w_f increases linearly with ligament length. A good linear regression with a high correlation coefficient ($r^2 \geq 90\%$) is achieved between the data for w_f and l for TPNR. However, linear regression confidence limits for kenaf composites with and without MAPP have been reduced to 78%.

By extrapolating the curve of w_f versus l to zero ligament length, value of the specific essential work of fracture (w_e) can be obtained at the y-axis intercept. The specific plastic work dissipation (βw_p) can then be calculated from the slope of the linear regression w_f versus l. The values of w_e and βw_p can be calculated according to Equation (3) as described

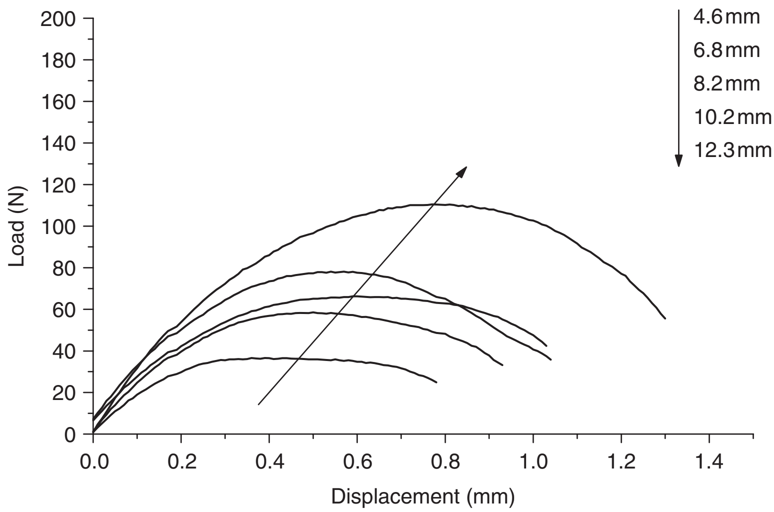

Figure 4. *Load–displacement curves for untreated TPNR/kenaf composites.*

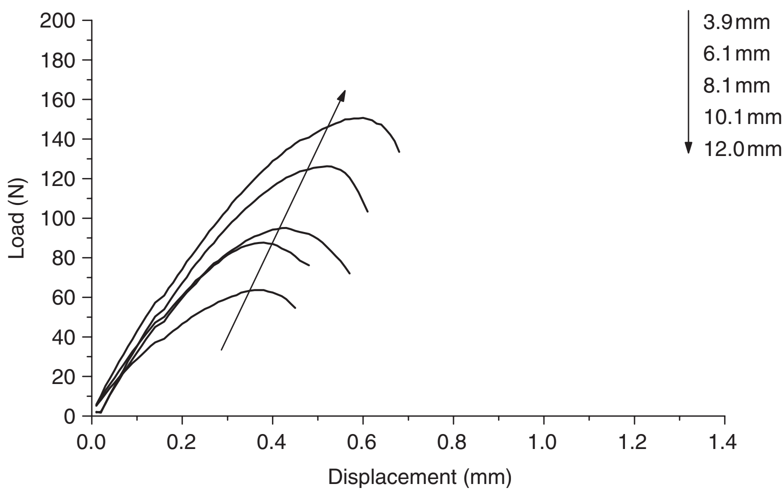

Figure 5. *Load–displacement curves for treated TPNR/kenaf composites.*

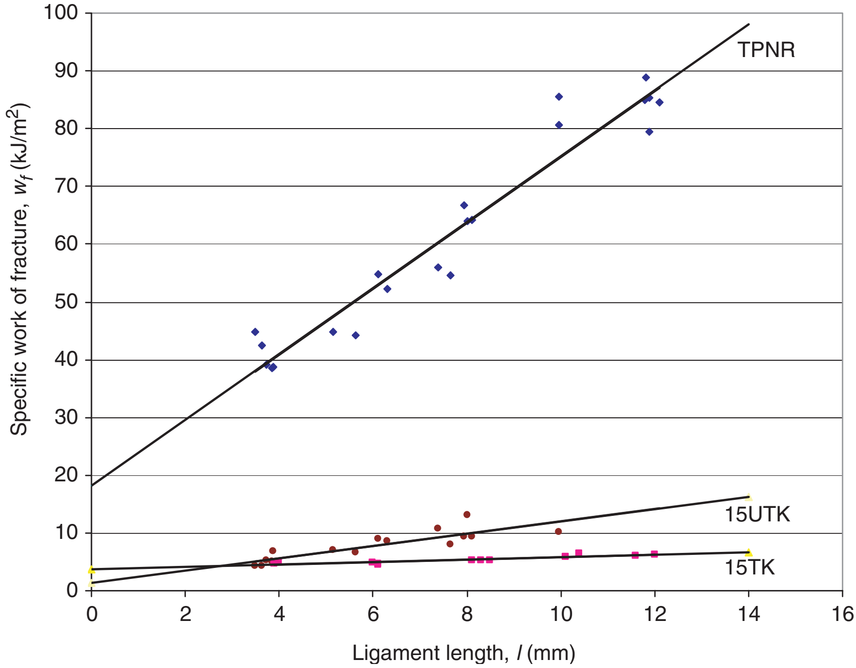

Figure 6. *Specific work of fracture (w_f) versus ligament length (l).*

Table 2. Summary of EWF results.

Composition (%)	w_e (kJ/m^2)	βw_p (kJ/m^2)	r^2
TPNR	16.0560	6.1130	0.9203
15 UTK	1.5268	0.7626	0.7815
15 TK	3.5043	0.2304	0.7863

in methodology. Details on the quantitative measurement of EWF results of TPNR and kenaf composites are summarized in Table 2, which shows that TPNR requires higher energy to initiate crack and its resistance to crack propagation was higher compared to the kenaf composites. As indicated in Table 2, extensive energy is dissipated in the outer plastic zone (βw_p) for TPNR matrix. Untreated TPNR/kenaf (UTK) composites show reduction in w_e and βw_p values, which are about 90% and 88%, respectively, compared to TPNR. However, in the TPNR–kenaf–MAPP (TK) system reduction in w_e was only about 78% as compared to TPNR. Thus this shows that the presence of MAPP has improved the w_e value by about 12% compared to untreated TPNR–kenaf. On the other hand, plastic deformation decreased in composites of TPNR–kenaf–MAPP as shown by the βw_p value.

Table 2 also shows that the presence of KF and coupling agent influenced the fracture behavior of TPNR blends and hybrid composites. Besides, the lower fracture toughness obtained in kenaf composites could be due to the nature of kenaf fiber and its random alignment in the TPNR matrix. The presence of fiber has changed the ductile behavior of TPNR to brittle fracture. The trend observed agreed well with the work of Tjong et al. [24]

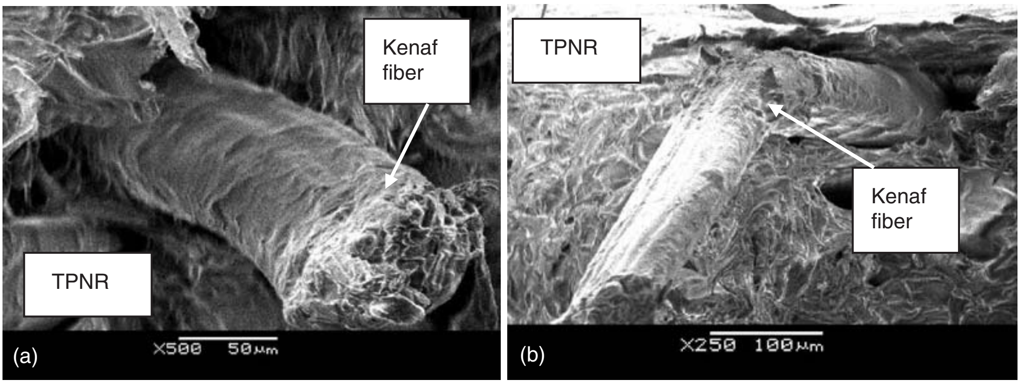

Figure 7. *SEM micrograph showing the fracture surface of UTK after EWF measurements.*

on styrene ethylene butadiene rubber (SEBS)/polypropylene/glass fiber hybrid composites, where fracture toughness was reduced by glass fiber addition. However, the results obtained show an opposite trend to another study by Tjong et al. [26] on short glass fiber (SGF)-reinforced polyamide 6,6 composites toughened with maleated SEBS where it was revealed that the w_e enhanced with SGF addition. It was also observed that matrix yielding, fiber debonding, and pullout are responsible for the energy absorption of hybrids containing SGF during EWF measurements.

The energy dissipated in the plastic zone of a polymer matrix involves microvoiding or cavitation (Tjong et al. [26]) of the elastomer and also necking and shear yielding of the matrix. However, the mechanisms decreased with the presence of KF in TPNR matrix. This is due to the fact that KF restrains the TPNR yielding in composites. Figure 7(a) and (b) shows a SEM micrograph of the fracture surface of TPNR–KF after EWF measurements. It is proved that plastic deformation occurs in the TPNR matrix of the hybrids, particularly in the matrix rich region next to the fiber ends. Moreover, debonding and the fiber pullout can also be observed in the fractographs. It is noted also formation of void at the end of KF pullout as in Figure 7(a) and fiber breakage in Figure 7(b) for TPNR–KF without MAPP have contributed to the failure mechanism. This indicates that matrix yielding (lower than in TPNR), fiber pullout, and fiber breakage are responsible for the energy absorption mechanisms.

In the case of the treated TPNR–kenaf composites, as observed in Figure 8(a) and (b), MAPP has been found to restrict matrix deformation. Accordingly, debonding and pullout of KF from the matrix are the primary energy absorption mechanisms for the composites during mode I (DENT samples) test loading.

Acoustic Emission (AE)

The dependence of the number of acoustic events and their amplitude distribution on the ligament length of DENT specimens was investigated. As seen in Figures 9–11, the amplitude histograms were between 21 and 55 dB (20 dB was the environmental signal threshold level), but their distribution varied depending on the material and range.

In the case of the TPNR matrix as in Figure 9, 70% of AE signals were lower than 25 dB. As reported by Czigany et al. [27] on polypropylene matrix, signals below 30 dB are

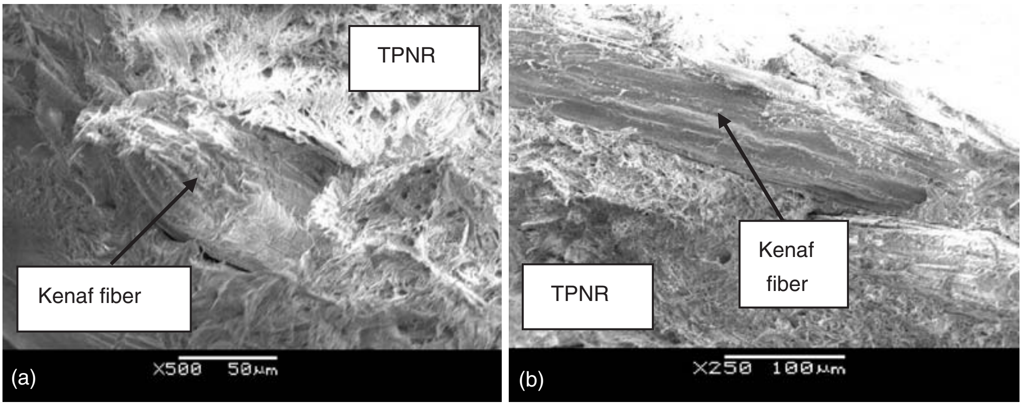

Figure 8. *SEM micrograph showing the fracture surface of TK after EWF measurements.*

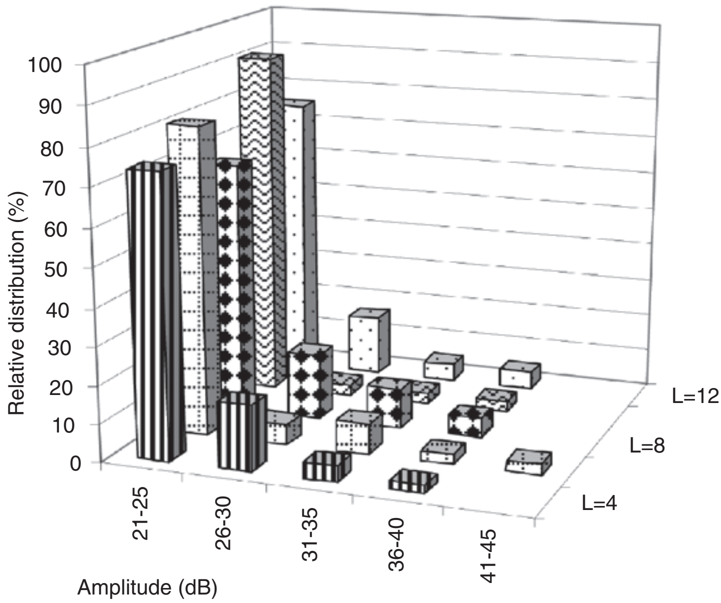

Figure 9. *Amplitude distributions of events of a TPNR matrix.*

referred to matrix deformation. It was also reported that signals with amplitudes above 40 dB before and after the maximum force refer to matrix cracking and tearing.

As for reinforced kenaf composites displayed in Figures 10 and 11, it is observed that the amplitude distributions of composites are greater than in the TPNR matrix. The highest amplitude recorded (55 dB) occurred in the case of untreated TPNR–KF, while the highest amplitude for TPNR–KF–MAPP was only at 50 dB. It can also be seen in Figures 10 and 11 that the amplitude lower than 25 dB has decreased from 70–90% for TPNR to between 40–60% for both types of kenaf composites. Accordingly, the fibers are found to cause the events, even though lower amplitudes were recorded compared to matrix failure.

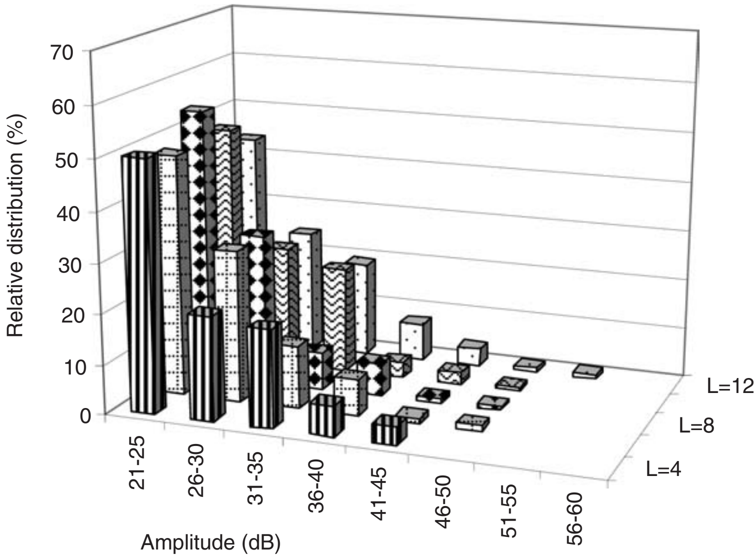

Figure 10. *Amplitude distribution of events in untreated TPNR–kenaf composites.*

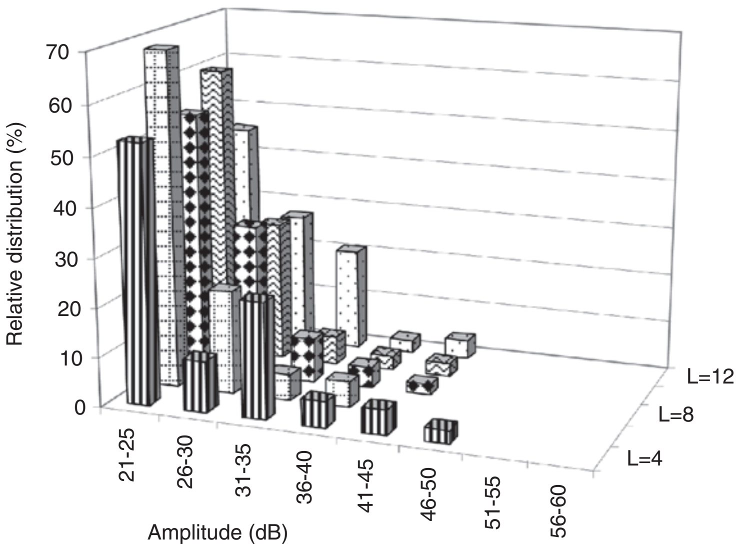

Figure 11. *Amplitude distribution of events in treated TPNR–kenaf composites.*

Based on Figure 9 it can be concluded that signals below 25 dB are derived from the failure of the matrix. The few larger signals originate from the final failure of the TPNR. As opposed to this, if Figures 10 and 11 are compared to Figure 9, it is obvious that the ratio of signals above 25 dB increases due to the fibers. These signals higher than 25 dB originate from fiber–matrix separation, fiber pullout, or fiber breakage.

Figure 12 shows an example of the force–elongation and amplitude–elongation plot of a TPNR–KF composite. The plot shows that the amplitude increases intermittently

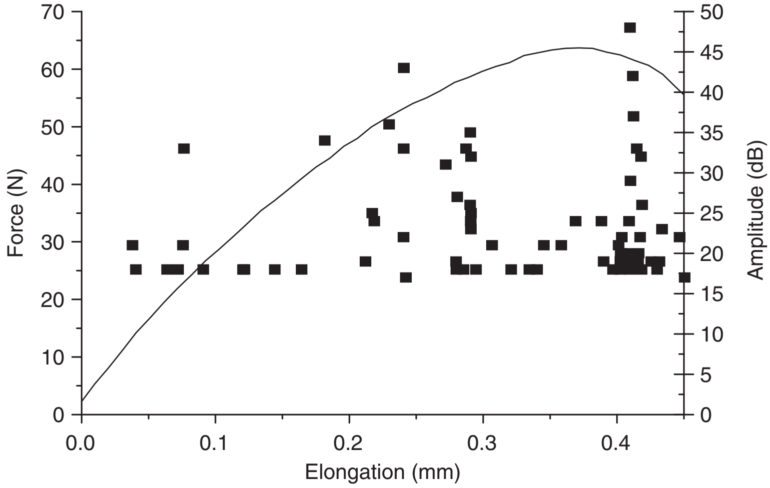

Figure 12. *Force and amplitude curve for treated TPNR–kenaf composite at 6 mm ligament length.*

with elongation. The 'bursts' of acoustic events could be associated with failure events in the composites. As shown in Figure 12, in the beginning, when the force is applied, only few AE signals are detected. However, at the middle of the process, the acoustic activity increases which can be associated to fiber–matrix debonding. It is also noted that near to the final fracture there is a second higher acoustic activity range which can be assigned to breakage of fiber. This observation agrees with previous studies by Dogossy and Czigany [28] who revealed that the amplitude detected in PE filled maize hull was characterized by matrix deformation (below 25 dB), fiber pullout (26–40 dB), and fiber breakage (over 41 dB). However, such a time-consuming calibration has not been carried out for this material. The calibration mentioned in Ref. [23] is a chapter of a PhD dissertation.

Only few signals are detected in the AE studies due to the fact that TPNR is a NR based material. The damping properties of NR could stabilize and neutralize the sound waves generated and propagating in the material and thus, the amplitude of AE signals reaching the sensor is much lower as compared to the source. Additionally, the low signals emitted in TPNR and TPNR–kenaf composites could be related to the sample dimension, which was very thin. The EWF theory is usually applied on thin foils by researchers. In the case of a thicker specimen, probably other fracture mechanical method could have been applied. It is generally known that thicker specimens tend to exhibit higher amplitude acoustic emission response.

From Figures 10 and 11, it can be seen that higher amplitude waves were emitted in the fractures below 25 dB. Therefore, this could suggest that matrix deformation contributed more to the failure processes. However, fiber pullout and breakage as observed under SEM micrographs in Figures 7 and 8 also contributed to the failure mechanisms.

Figure 13 shows the average number of AE event counts for various ligament lengths ranging from 4 to 12 mm. The average number of AE event counts was based on 20–60 dB signals. Five specimens were evaluated for each ligament length. As shown in Figure 13, the average number of AE event counts for TPNR matrix for the whole series of ligament lengths was around 40–50. The second bar with gray color refers to UTK. Figure 13 demonstrated that the presence of kenaf fiber (treated and untreated fibers) has increased

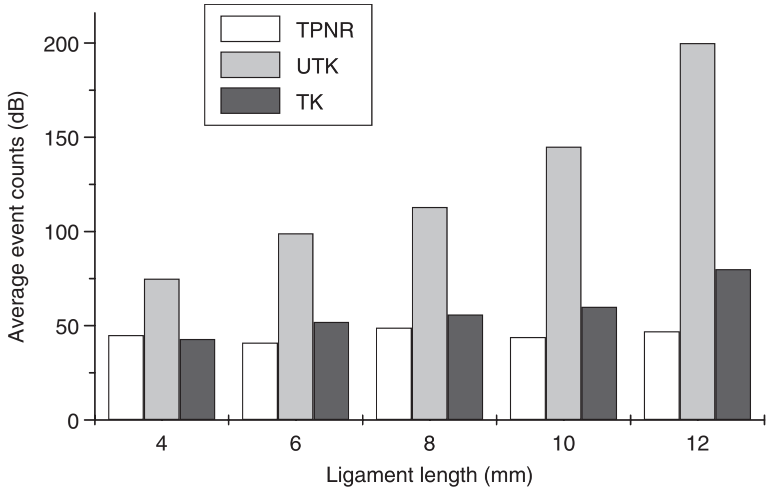

Figure 13. *Average event counts versus ligament length of TPNR, UTK, and TK.*

the AE event counts compared to TPNR. The higher the ligament length, the higher the number of AE event counts for UTK composites. The higher event counts in the case of the composite as compared to the TPNR matrix revealed that, apart from matrix deformation, the failure was also caused by the fiber failure due to higher event counts in the case of a composite compared to a TPNR matrix. However, lower signals of AE event were recorded for TK compared to UTK composites. Based on Figure 13, by making comparison at 12 mm ligament length, the average number of AE event counts for UTK was almost 150% higher than for TK. This could be related to a stick-slip mechanism caused by the rough nature of kenaf fiber. The rough surface of kenaf fiber prevents it from being directly pulled out from the matrix and thus it would emit higher signal during pullout failure. As for untreated TPNR–kenaf, pullout is more dominant and this has been proven in Figure 9 where the range of 26–40 dB show higher amplitude. However, an addition of MAPP has improved the adhesion between matrix and fiber as described elsewhere [29], consequently resulting in less fiber pullout as depicted in Figure 11.

CONCLUSION

The TPNR and TPNR–KF composites have been successfully evaluated using the EWF method. TPNR shows higher w_e and βw_p values than its composites. The presence of kenaf fiber (treated and untreated fiber) has restricted the yielding of the matrix and changed the ductile failure of TPNR to brittle fracture. From the AE analysis, higher signals were emitted in case of kenaf composites. It was found that lower value of w_e in EWF measurement, resulted in more AE signals, and vice versa. (Direct correlation could not be found between βw_p and AE signals, since βw_p is referred to plasticity of polymer). In order to be able to generalize the conclusion, measurement has to be carried out and verified for other materials as well. Based on AE signals together with the information gained from EWF and SEM observation, failure mechanism could be associated to matrix deformation, fiber pullout, and fiber breakage.

ACKNOWLEDGMENTS

The author wish to thank the International Islamic University Malaysia, Public Services Department, Universiti Kebangsaan Malaysia, grant 09-02-02-0074 under the Ministry of Science & Technology, Yayasan Felda, Science University of Malaysia and the Hungarian Scientific Research Fund (OTKA K 61424 and NI 62729), further GVOP-3.1.1-2004-05-0531/3.0.

REFERENCES

1. Sulaiman, C.S., Ahmad, S.H. and Abdullah, I. (1994). Kajian Adunan Getah Asli/Polietilena Berketumpatan Tinggi Dengan Getah Asli Cecair Sebagai Penserasi, *Sains Malaysiana*, **23**: 29–38.
2. Nair, K.C.M., Diwan, S.M and Thomas, S. (1996). Tensile Properties of Short Sisal Fibre Reinforced Polystyrene Composites, *J. Appl. Polym. Sci.*, **60**: 1483–1497.
3. Rowell, R.M., Sanadi, A., Jacobson, R. and Caulield, D. (1999). *Kenaf Properties, Processing and Products*, Mississippi State University, Ag. & Bio. Eng., 381–392.
4. Mai, Y.-W. and Powell, P.J. (1991). Essential Work of Fracture and J-integral Measurements for Ductile Polymers, *J. Polym. Sci., Part B*, *Polym. Phys.*, **29**(7): 785–793.
5. Mai, Y.-W., Wong, S.-C. and Chen, X.-H. (1999). Application of Fracture Mechanics for Determination of Toughness of Polymer Blends (chap. 20). Di dalam, In: Paul, D.R. and Bucknall, C.B. (eds), *Polymer Blends: Formulations and Performance*, Vol. 2, pp. 17–58, Wiley, New York.
6. Mai, Y.-W., Wong, S.C. and Chen, X.H. (2000). Application of Fracture Mechanics for Characterization of Toughness of Polymer Blends in Polymer Blends, In: Paul, D.R. and Bucknall C.B. (eds), *Performance*, Wiley, New York.
7. Moore, D.R., Pavan, A. and Williams, J.G. (2001). Fracture Mechanics Testing Methods for Polymers, Adhesives and Composites, *ESIS Publication 28*. Elsevier, Netherlands.
8. Gong, G., Xie, B.-H., Yang, W., Li, Z.-M., Zhang, W.-Q. and Yang, M.-B. (2005). Essential Work of Fracture (EWF) Analysis for Polypropylene Grafted with Maleic Anhydride Modified Polypropylene/Calcium Carbonate Composites, *Polym. Testing*, **24**: 410–417.
9. Mouzakis, D.E., Gahleitner, M. and Karger-Kocsis, J. (1998). Toughness Assessment of Elastomeric Polypropylene (ELPP) by the Essential Work of the Fracture Method, *J. Appl. Polym. Sci.*, **70**: 873–881.
10. Karger-Kocsis, J., Czigany, T. and Moskala, E.J. (1997). Thickness Dependence of Work of Fracture Parameters of an Amorphous Copolyester, *Polymer*, **38**: 4587–4593.
11. Maspoch, M.L.I., Games-Perez, J. and Karger-Kocsis, J. Effects of Thickness, Deformation Rate and Energy Partitioning on the Work of Fracture Parameters of uPVC Films, *Polym. Bull.*, **50**: 279–286.
12. Karger-Kocsis, J. and Czigany, T. (2000). Strain Rate Dependence of the Work of Fracture Response of an Amorphous Poly(ethylene-naphthalate) (PEN) Film, *Polym. Eng. and Sci.*, **40**(8): 1809–1815.
13. Karger-Kocsis, J., Czigany, T. and Moskala, E.J. (1998). Deformation Rate Dependence of the Essential and Non-essential Work of Fracture Parameters in an Amorphous Copolyester, *Polymer*, **39**(17): 3939–3944.
14. Wu, J.-S., Mai, Y.-W. and Cotterell, B. (1993). *J. Mater. Sci.*, **28**(12): 3373–3384.
15. Ferrer-Balas, D., Maspoch, M.L.I., Martinez, E. Ching, Li, R.K.Y. and Mai, Y.-W. (2001). Influence of Annealing on the Microstructural, Tensile and Fracture Properties of Polypropylene Films, *Polym.*, **42**(6): 2665–2674.
16. Yamakawa, R.S., Razzino, C.A., Correa, C.A. and Hage Jr., E. (2004). Influence of Notching and Moulding Conditions on Determination of EWF Parameters in Polyamide 6, *Polymer Testing*, **23**: 195–202.

17. Karger-Kocsis, J., Barany, T. and Moskala, E.J. (2003). Plane Stress Fracture Toughness of Physically Aged Plasticized PETG as Assessed by the Essential Work of Fracture (EWF) Method, *Polymer*, **44**: 5691–5699.
18. Fayolle, B., Tcharkhtchi, A. and Verdu, J. (2004). Temperature and Molecular Weight Dependence of Fracture Behaviour of Polypropylene Films, *Polym. Testing*, **23**: 939–947.
19. Karger-Kocsis, J. and Moskala, E.J. (2000). Molecular Dependence of the Essential and Non-essential Work of Fracture of Amorphous Films of Poly(ethylene-2,6-napthalate) (PEN), *Polymer*, **41**: 6301–6310.
20. Czigany, T., Marosfalvi, J. and Karger-Kocsis, J. (2000). An Acoustic Emission Study of the Temperature-dependent Fracture Behavior of Polypropylene Composites Reinforced by Continuous and Discontinuous Fiber Mats, *Compos. Sci. & Technol.*, **60**: 1203–1212.
21. Abdullah, I. and dan Zakaria, Z. (1989). Pendepolimeran Fotokimia Getah Asli, *Sains Malaysiana*, **18**(2): 99–109.
22. Mai, Y.W. and Cotterell, B. (1986). On the Essential Work of Ductile Fracture in Polymers, *Int. J. Fract.*, **32**(2): 105–125.
23. Wu, J.S. and Mai, Y.-W. (1996). The Essential Fracture Work Concept for Toughness Measurement of Ductile Polymers, *Polym. Engr. Sci.*, **36**(18): 2275–2288.
24. Tjong, S.C., Xu, S.-A., Li, R.K.-Y. and Mai, Y.-W. (2002). Mechanical Behavior and Fracture Toughness Evaluation of Maleic Anhydride Compatibilized Short Glass Fiber/SEBS/Polypropylene Hybrid Composites, *Compos. Sci. & Technol.*, **62**: 831–840.
25. Li, W.D., Li, R.K.Y. and Tjong, S.C. (1997). Fracture Toughness of Elastomer-modified Polypropylene, *Polym. Testing*, **16**: 563–574.
26. Tjong, S.C., Xu, S.-A., Li, R.K.-Y. and Mai, Y.-W. (2002). Short Glass Fiber-reinforced Polyamide 6,6 Composites Toughened with Maleated SEBS, *Compos. Sci. & Technol.*, **62**: 2017–2027.
27. Czigany, T. (2005). Special Manufacturing and Characteristics of Basalt Fiber Reinforced Hybrid Polypropylene Composites: Mechanical Properties and Acoustic Emission Study, *Compos. Sci. & Technol.*, **66**(16): 3210–3220.
28. Dogossy, G. and Czigany, T. (2006). Failure Mode Characterization in Maize Hull Filled Polyethylene Composites by Acoustic Emission, *Polym. Testing*, **25**: 353–357.
29. Kishi, H., Yoshioka, M., Yamanoi, A. and Shiraishi, N. (1988). Composites of Wood and Polypropylenes I, *Mokuzai Gakkaishi*, **34**(2): 133–139.